Journal of Advances and Scholarly Researches in Allied Education
Vol. 16, Issue No. 6, May-2019, ISSN 2230-7540

Design of Novel Biorthogonal Wavelets

Padmashri Dhanashire[1]* Dr. Tryambk Hirwarkar[2]

[1] Research Scholar, Department of Electronics & Communication Engineering, Sri Satya Sai University of Technology & Medical Sciences, Sehore, M.P.

[2] Research Guide, Department of Electronics & Communication Engineering, Sri Satya Sai University of Technology &Medical Sciences, Sehore, M.P.

Abstract – This paper describes the properties of wavelets. The properties and features of conventional wavelets are mentioned. The need of biorthogonal and the concept of biorthogonal wavelets are presented. Though a large number of wavelet functions exist, a specific application may require specialized wavelets in terms of shape, size and smoothness to fulfill the applications' requirements. In this paper, four new functions were generated and used to represent image data for compression. New conventional biorthogonal wavelets are proposed. The simulation results of the Image compression using new conventional wavelets technique are presented in this paper.

---------------------------------X--------------------------------

1. INTRODUCTION

A large number of test images are considered to validate the performance of the proposed wavelets. These images include medical images, photographic images, satellite images both gray scale and color images. The multi-resolution signal decomposition was first described by Stephen G. Mallat in 1989. [1] designated a mathematical prototype for the computation and analysis of the concept of a multi-resolution illustration. He has clarified how to excerpt the difference of data between consecutive resolutions and consequently define a novel representation called the wavelet representation. This wavelet representation is calculated by decomposing the original signal using an orthonormal basis, and can be understood as a decomposition using a set of self-governing frequency channels having a spatial alignment tuning.

The theory of wavelet can be imagined as a research of finding functions that act as wavelets. It is not just acting as wavelets but also to represent the input data in a suitable form to apply different tasks. The aim is to discover functions which are concurrently localized in both time and frequency (within the limits levied by the Heisenberg principle). The wavelet theory seeks functions that can approximate functions as competently as possible, with as few coefficients as possible, as just described. One has to have different features for a given application to satisfy the criteria of the application. Few of them can be complimentary to each other, so the designer has to pick one of the properties to satisfy based on the application. The features of their "quadrature mirror philtres", 'H' and "H" are used to design wavelets. 'G'. Here are a few significant property listings.

► Compact Support

This property is vital for numerical applications like implementation of the finite impulse response and fast wavelet transform (FWT). It is also useful in terms of sensing point-wise singularities. If a signal 'g' has a singularity at 'n0' then if 'n0' is inside the support of '*ψ*j,n', the respective coefficient will become huge. If the wavelet function '*ψ'* has support of '*l*', then at each scale 'j' there will be '*l*' wavelets intermingling with the singularity (this mean that their support contains 'n0'). Shorter the support, the less is wavelets intermingling with the singularity.

Compact support of the scaling function ' I I ' accords with finite impulse response, furthermore when the low pass filter is supported on say [N1, N2], as is ' I I ', and it is easy to see that the wavelet function '*ψ'* having support of the length (N2 – N1).

► Smoothness

The smoothness of the wavelet functions has a remarkable effect on the error led by thresholding / quantizing the wavelet coefficients. The smoother the wavelet longer is the support. For example an error '□' is added to the coefficient $\langle f, \psi_{j,k} \rangle$ it means that add an error '□*ψ*j,k' is added to the reconstruction. Flat or smooth errors are frequently less visible in case of images and videos and less audible in case of audio and video.

► **Vanishing Moments**

A wavelet function '*ψ*' has 'M' number of vanishing moments if

$$\int_{-\infty}^{\infty} \psi(x)\, x^m dx = 0, \qquad m = 0, 1, \ldots\ldots, M-1. \qquad \ldots\ldots(1)$$

The equation 1 indicates that the wavelet function '*ψ*' is orthogonal to polynomials xm of degree 'M – 1'. Wavelets are typically designed with vanishing moments, which result in wavelets orthogonal to the low degree polynomials, and tends to compress non-oscillatory signals. For instance an M-differentiable function '*f*' can be expanded in a Taylor series

$$f(x) = f(0) + f'(0)x + \ldots\ldots\ldots + f^{(M-1)}(0)\frac{x^{M-1}}{(M-1)!} + f^{(M)}(\xi(x))\frac{x^M}{M!} \qquad \ldots\ldots(2)$$

and conclude, if the wavelet function '*ψ*' has 'M' vanishing moments such that

$$|\langle f, \psi\rangle| \le \max_x \left| f^{(M)}(\xi(x))\frac{x^M}{M!} \right|. \qquad \ldots\ldots(3)$$

On the other side, the fact that a wavelet function '*ψ*' has 'M' vanishing moments is an outcome of the following identity being valid for the filter 'G.

$$\sum_k G(k)\, k^m = 0, \qquad m = 0, 1, \ldots\ldots\ldots, M-1. \qquad \ldots\ldots(4)$$

The number of vanishing moments of the wavelet function '*ψ*' depends on the number of vanishing derivatives of which is again related to the number of vanishing derivatives of the refinement mask

$$\hat{\psi}(\xi) \text{ at } \xi = 0.$$

The above relationships suggest that if the wavelet function '*ψ*' has 'M' vanishing moments, then the polynomials of degree 'M – 1' are replicated by the scaling functions, this is often denoted as the approximation order of the multiresolution analysis. Haar wavelet has M = 1, so only constant functions are reproduced by the scaling functions.

The conditions imposed on orthogonal wavelets imply that if the wavelet function '*ψ*' has 'M' vanishing moments then its support is minimum '2M – 1'. For a given number of vanishing moments, the Daubechies wavelets have the least support. There is also a tradeoff between the moments of absence and the period of assistance. If the function between singularities is smooth and has few singularities, so one can take advantage of the moments that disappear. One might opt to use wavelets with little support if there are several singularities. The 0s of the refinement mask at z = -1 are related to both vanishing moments and smoothness. Although it is the number of vanishing moments that determine their size on fine scales, not the regularity, in terms of amplitude coefficients.

► **Symmetry**

It is not possible to build symmetric compactly supported orthogonal wavelets other than Haar. Because the symmetry is useful for signal and image processing applications the standard wavelets are designed with closely or nearly symmetric. It can be attained at the cost of other properties. If orthogonality is given up then there are smooth, symmetric and compactly supported biorthogonal wavelets.

2. BI-ORTHOGONAL WAVELETS

As an orthogonal wavelet, bi-orthogonal wavelets have much of the features, but the bi-orthogonal wavelets have the benefit of providing more design choices, while the orthogonal wavelet has only one design case for each length. As well as asymmetric, bi-orthogonal wavelets may be symmetrical. A broad collection is generated by asymmetric bi-orthogonal wavelets as the design equations obtained from other properties would be greater than scaling or wavelet function coefficients. They are correlated with ideal philtre banks for analysis and restoration. A generalisation of orthogonal wavelets is defined by bi-orthogonal wavelets. In bi-orthogonal wavelets, a pair of dual bi-orthogonal base functions are used instead of a single orthogonal base function; one for the step of analysis and the other for the step of synthesis.

The two pairs of wavelet and scaling functions, *'φ', 'ψ'* and $\tilde{\phi}, \tilde{\psi}$ are defined recursively by the two pairs of filters '*m*0', '*m*1', and *m*0 , *m*1 . In the frequency domain *m*0 , *m*1. In the frequency domain these relations are

$$\tilde{\phi}(w) = m_0(w/2)\,\tilde{\phi}(w/2), \quad \tilde{\psi}(w) = m_1(w/2)\,\tilde{\phi}(w/2)$$

$$\tilde{\tilde{\phi}}(w) = \hat{m}_0(w/2)\,\tilde{\tilde{\phi}}(w/2), \quad \tilde{\tilde{\psi}}(w) = \hat{m}_1(w/2)\,\tilde{\tilde{\phi}}(w/2)$$

Where

$$m_0(w) = \frac{1}{\sqrt{2}}\sum_k h_k e^{-ikw}, \quad m_1(w) = \frac{1}{\sqrt{2}}\sum_k g_k e^{-ikw}$$

$$\tilde{m}_0(w) = \frac{1}{\sqrt{2}}\sum_k \tilde{h}_k e^{-ikw}, \quad \tilde{m}_1(w) = \frac{1}{\sqrt{2}}\sum_k \tilde{g}_k e^{-ikw}$$

The bi-orthogonality condition in the frequency domain is equal to

$$\sum_k \tilde{\tilde{\phi}}(w+k2\pi)\ \tilde{\phi}'(w+k2\pi)=1$$
$$\sum_k \tilde{\tilde{\psi}}(w+k2\pi)\ \tilde{\psi}'(w+k2\pi)=1$$
$$\sum_k \tilde{\tilde{\psi}}(w+k2\pi)\ \tilde{\phi}'(w+k2\pi)=0$$
$$\sum_k \tilde{\tilde{\phi}}(w+k2\pi)\ \tilde{\psi}'(w+k2\pi)=0$$

For all w E R

This means that the filters 'm_0', 'm_1' and their duals *m*0 $\tilde{m}_0$, $\tilde{m}_1$ have to satisfy

$$\tilde{m}_0(w)\tilde{m}_0'(w)+\tilde{m}_0(w+\pi)\tilde{m}_0'(w+\pi)=1$$
$$\tilde{m}_1(w)\tilde{m}_1'(w)+\tilde{m}_1(w+\pi)\tilde{m}_1'(w+\pi)=1$$
$$\tilde{m}_1(w)\tilde{m}_0'(w)+\tilde{m}_1(w+\pi)\tilde{m}_0'(w+\pi)=0$$
$$\tilde{m}_0(w)\tilde{m}_1'(w)+\tilde{m}_0(w+\pi)\tilde{m}_1'(w+\pi)=0$$

The above equations can be written in matrix form as

$$\begin{pmatrix}\tilde{m}_0(w) & \tilde{m}_0(w+\pi)\\ \tilde{m}_1(w) & \tilde{m}_1(w+\pi)\end{pmatrix}\begin{pmatrix}m_0(w) & m_1(w)\\ m_0(w+\pi) & m_1(w+\pi)\end{pmatrix}' = \begin{pmatrix}1 & 0\\ 0 & 1\end{pmatrix}$$

Or,

$$\tilde{M}(w)[M^T(w)]' = I$$

where M is the modulation matrix

$$M=\begin{pmatrix}m_0(w) & m_0(w+\pi)\\ m_1(w) & m_1(w+\pi)\end{pmatrix}$$

and I is the identity matrix.

3. NOVEL BI-ORTHOGONAL WAVELETS

Though a large number of wavelet functions exist, a specific application may require specialized wavelets in terms of shape, size and smoothness to fulfill the applications' requirements. In this paper, four new functions will be generated and will be used to represent image data for compression. Orthogonal wavelets are one of the elementary groups of wavelets. But it is difficult to provide an orthogonal wavelet that needs perfect reconstruction of a symmetric property. Therefore, orthogonal and symmetric increases are a must. The solution was in the form of bi-orthogonal wavelets that preserved a perfect state of reconstruction. Although the literature proposes a number of bi-orthogonal wavelets, four new bi-orthogonal wavelets are proposed in this paper, providing better compression efficiency. Biorthogonal wavelet architecture is concerned with creating two sets of functions with specific properties. The two sets can be used one in one,

Decomposition and others in the process of wavelet transformation reconstruction.

Since $\int \phi(t)\tilde{\phi}(t-k)\,dt=\delta_{k,0}$

$$\sum_n h(n)\,\tilde{h}(n-2k)=\delta_{k,0} \qquad \text{..........................(3.1)}$$

i.e., h(n) is orthogonal to even translates of itself. Here $\tilde{h}$ is orthogonal to h. Now let the positioning of $\phi(t)$ and $\tilde{\phi}(t)$ is from *N*1 to *N*2 and $\tilde{N}_1$ to $\tilde{N}_2$ respectively. Equation (3.1) implies

$$N_2-\tilde{N}_1=2p \text{ and } \tilde{N}_2-N_1=2\tilde{p}+1,\ p,\tilde{p}\in Z \qquad \text{..............(3.2)}$$

The positioning of the scaling function coefficients is very important. This decides the constraints on coefficients. If equation (3.2) is not satisfied there will be no feasible solution for $\tilde{h}(k)$ coefficients. The proper positioning was identified and it was found that for the following values the solution is feasible.

$$N_1=-3,\ \ N_2=1 \text{ and } \tilde{N}_1=-3,\ \ \tilde{N}_2=4 \qquad \text{.............................(3.3)}$$

Now apply the conditions on coefficients. The equation $\int\tilde{\phi}(t)\,dt=1$

results in $\sum_k \tilde{h}(k)=\sqrt{2}$ hence

$$\tilde{h}(-3)+\tilde{h}(-2)+\tilde{h}(-1)+\tilde{h}(0)+\tilde{h}(1)+\tilde{h}(2)+\tilde{h}(3)+\tilde{h}(4)=\sqrt{2} \qquad \text{...........(3.4)}$$

Now use equation (3.4), i.e.,

$$\sum_n h(n)\,\tilde{h}(n-2k)=\delta_{k,0}$$

Substituting k = 0 in

$$\sum_n h(n)\,\tilde{h}(n-2k)=\delta_{k,0}\ ,$$

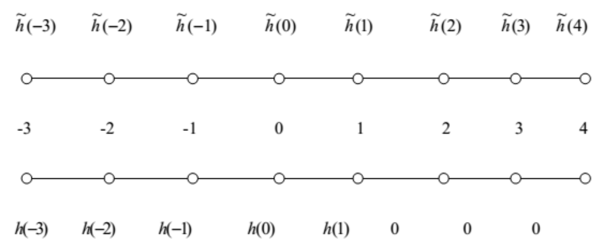

$$h(-3)\tilde{h}(-3)+h(-2)\tilde{h}(-2)+h(-1)\tilde{h}(-1)+h(0)\tilde{h}(0)+h(1)\tilde{h}(1)=1 \qquad \text{.........................(3.5)}$$

Substituting

$$k=-1 \text{ in } \sum h(n)\,\tilde{h}(n-2k)=\delta_{k,0}\ ,$$

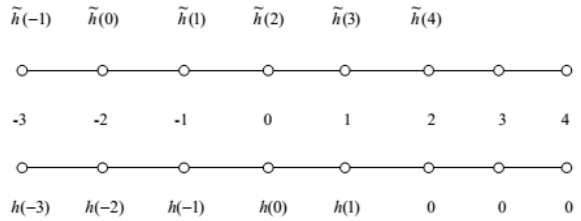

$$h(-3)\tilde{h}(-1)+h(-2)\tilde{h}(0)+h(-1)\tilde{h}(1)+h(0)\tilde{h}(2)+h(1)\tilde{h}(3)=0 \quad \text{.........................(3.6)}$$

Substitute

$$\mathrm{k}=1 \text{ in } \sum_{n} h(n)\,\tilde{h}(n-2k)=\delta_{k,0}\ ,$$

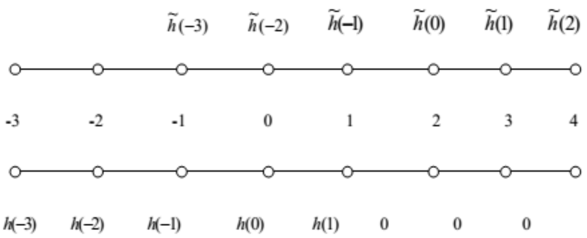

$$h(-1)\tilde{h}(-3)+h(0)\tilde{h}(-2)+h(1)\tilde{h}(-1)=0 \quad \text{.....................................(3.7)}$$

Substituting

$$\mathrm{k}=-2 \text{ in } \sum h(n)\,\tilde{h}(n-2k)=\delta_{k,0}\ ,$$

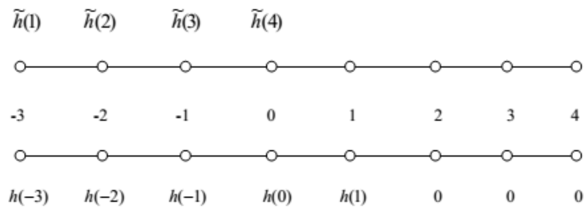

$$h(-3)\tilde{h}(1)+h(-2)\tilde{h}(2)+h(-1)\tilde{h}(3)+h(0)\tilde{h}(4)=0 \quad \text{...................................(3.8)}$$

Substituting

$$\mathrm{k}=-3 \text{ in } \sum_{n} h(n)\,\tilde{h}(n-2k)=\delta_{k,0}\ ,$$

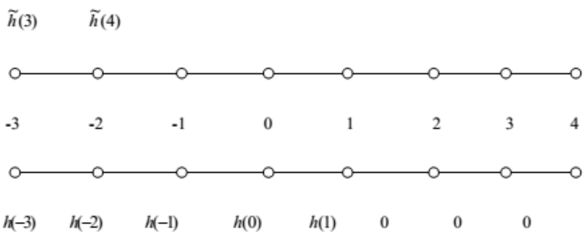

$$h(-3)\tilde{h}(3)+h(-2)\tilde{h}(4)=0$$

....(3.9)

Nbior1:

The general form of Spline of order k is given by :

$$N_k(t)=\sum_{i=0}^{k} p_i N_k(2t-i)$$

Where

$$p_i=\frac{1}{2^{k-1}}\binom{k}{i}$$

Consider Spline of order 4 which is given below :

$$N_4(t)=\frac{1}{8}N_4(2t)+\frac{4}{8}N_4(2t-1)+\frac{6}{8}N_4(2t-2)+\frac{4}{8}N_4(2t-3)+\frac{1}{8}N_4(2t-4)$$

The above spline is considered as one of the scaling function.

Hence the un-normalized coefficients becomes,

$$\frac{1}{8},\frac{4}{8},\frac{6}{8},\frac{4}{8}\ and\ \frac{1}{8}.$$

The sum of normalized coefficients must be equal to $\sqrt{2}$ this follows from the requirement

$$\int \phi(t)dt=1.$$

Therefore,

$$a\left(\frac{1}{8}+\frac{4}{8}+\frac{6}{8}+\frac{4}{8}+\frac{1}{8}\right)=\sqrt{2} \quad \Rightarrow a=\frac{1}{\sqrt{2}}$$

Hence the normalized coefficients of $\phi(t)$ are :

$$\frac{1}{8\sqrt{2}},\frac{4}{8\sqrt{2}},\frac{6}{8\sqrt{2}},\frac{4}{8\sqrt{2}}\ and\ \frac{1}{8\sqrt{2}}.$$

Using equation (5.7), the scaling coefficients becomes

$$h(-3)=\frac{1}{8\sqrt{2}},h(-2)=\frac{4}{8\sqrt{2}},h(-1)=\frac{6}{8\sqrt{2}},h(0)=\frac{4}{8\sqrt{2}}\ and\ h(1)=\frac{1}{8\sqrt{2}}. \quad \text{.......(3.10)}$$

Using equations (3.5) to (3.10), the values of the coefficients are calculated and given below

~(-3)	~(-2)	~(-1)	~(0)	~(1)	~(2)	~(3)	~(4)
0.1426	0.8244	-.0929	0.2413	0.1043	0.2275	-0.076	0.0532

Already the scaling function coefficients are assumed to be that of splines of order 4 and the positioning is given by N1 and N2, i.e.,

h(-3)	h(-2)	h(-1)	h(0)	h(1)
0.0883	0.3535	0.5303	0.3535	0.0883

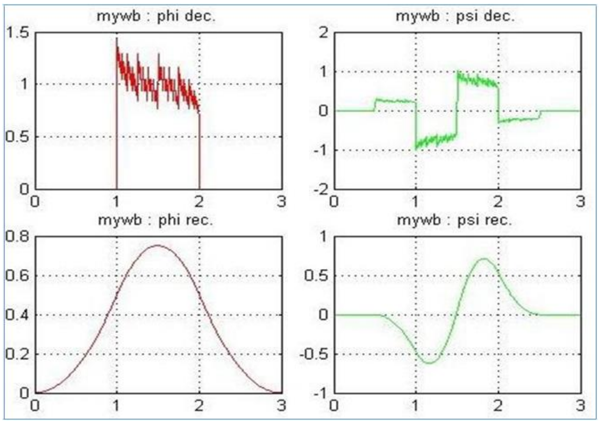

Fig. 4.1 Scaling and Wavelet Functions of the Wavelet NBior1

In the same way three more wavelets are designed by considering the variations of spline as one of scaling functions. The 'φ' and 'ψ' functions associated with new wavelets are plotted in the figures 4.2, 4.3, and 4.4 respectively.

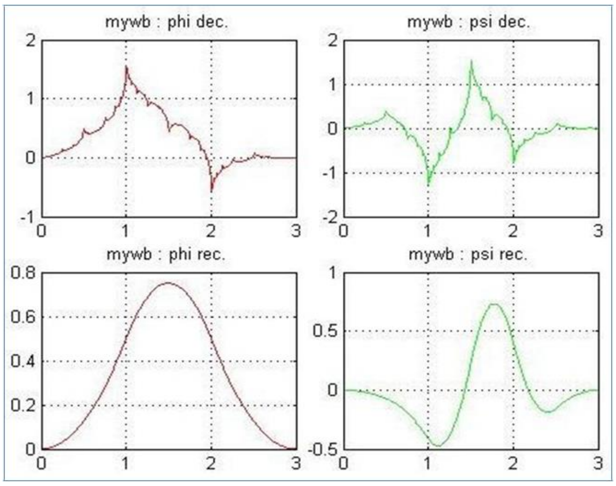

Fig. 4.2 New Wavelets: phi, psi functions associated with NBior2

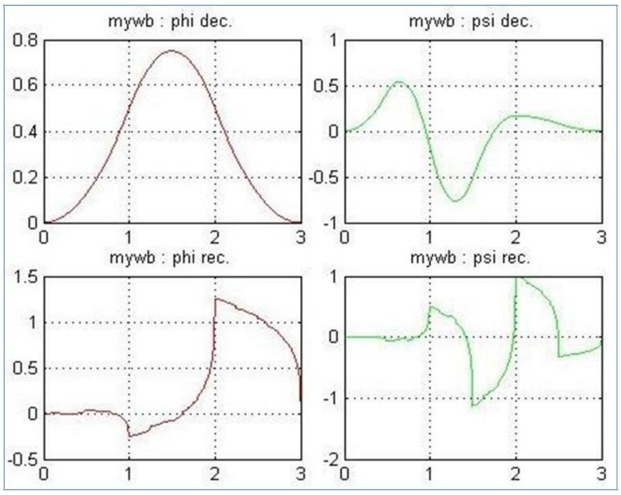

Fig. 4.3 New Wavelets: phi, psi functions associated with NBior3

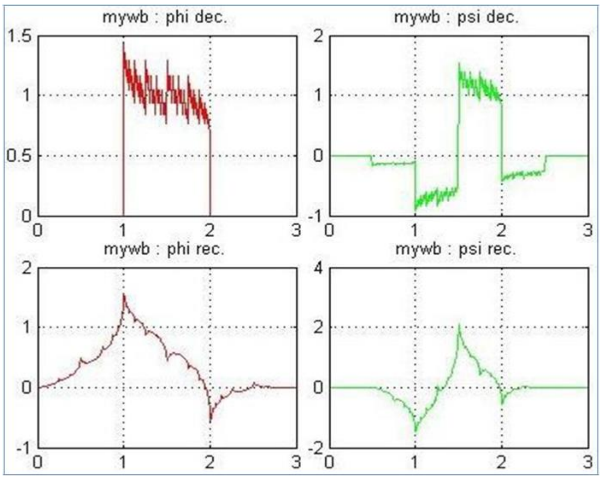

Fig. 4.4 New Wavelets: phi, psi functions associated with NBior4

Table 4.1 The Scaling and Wavelet function coefficients of new wavelets

NBior 1	Non-zero low-pass coefficients	0.1426 0.8244 -0.0929 0.2413 0.1043 0.2275 -0.0761 0.0532
	Non-zero high-pass coefficients	**0.0532 0.0761 0.2275 -0.1043 0.2413 0.0929 0.8244 -0.1426**
NBior 2	Non-zero low-pass coefficients	1.4154 -0.3471 0.3914 0.0425 -0.1265 0.0164 0.0235 -0.0014
	Non-zero high-pass coefficients	**-0.0014 -0.0235 0.0164 0.1265 0.0425 -0.3914 -0.3471 -1.415**
NBior 3	Non-zero low-pass coefficients	0.0034 0.9312 -0.1256 0.4788 0.1011 0.0633 -0.0352 -0.0028
	Non-zero high-pass coefficients	**-0.0028 0.0352 0.0633 -0.1011 0.4788 0.1256 0.9312 -0.0034**
NBior	Non-zero low-pass coefficients	0.9713 0.3791 0.1742 -0.0988 -0.0282 0.0123 0.0051 -0.0008
	Non-zero high-pass coefficients	**-0.0008 -0.0051 0.0123 0.0282 -0.0988 -0.1742 0.3791 -0.971**

Hence the design of new biorthogonal wavelet is done. The design steps can be listed as given below.

i. First fix the lengths N_1, N_2, $\tilde{N}_1$ and $\tilde{N}_2$ by taking equation (4.6) into consideration

ii. Shape the equations corresponding to the properties on the decomposing and interpretation side in terms of scaling and wavelet functions.

iii. Then take from a regular one of the base functions or a variant of a standard function.

iv. After replacing the corresponding values in the equations developed in phase ii, the final equations are obtained solely in terms of one function

v. Then solve the equations. (The equations are solved using 'solve' of Symbolic Math Toolbox in MATLAB). Hence the coefficients of the scaling and wavelet functions are obtained.

vi. Add the designed wavelets to the MATLAB (using 'wavemngr' of Wavelet Toolbox).

vii. Then the designed wavelets have to be applied for transformation and inverse transformation of an image and verify the perfect reconstruction (using 'dwt2', 'idwt2' and 'measerr' of Wavelet Toolbox)

The key point in this analysis is how the coefficients of one of the basic functions can be taken. The variations of the spline feature are taken into account for that reason here. The remaining set of coefficients is determined by taking one set of coefficients from combinations of the spline equation. Since the equations are generated by taking the properties into account, the necessary wavelets will obviously be built when the equations are solvable.

4. IMAGE COMPRESSION BY USING NOVEL CONVENTIONAL WAVELETS

4.1 Simulation Results

In this section, the compression performance of SPIHT using proposed wavelets is presented. Two categories of images are considered: multi-gray level and binary images. In the first category both gray scale and colour images are considered.

PSNR and CR values obtained with new wavelets on multi-gray level images are given in the tables 4.2, 4.3, 4.4 and 4.5 respectively. The screen shots of the compression performance of new conventional wavelets is given in the figures 4.5 to 4.10.

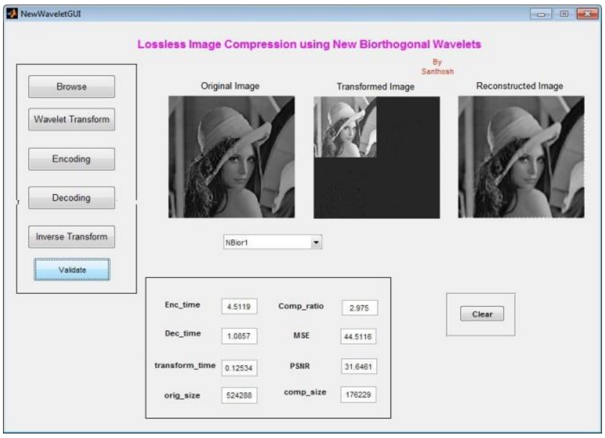

Fig. 4.5 Compression of 'lena.jpg' using NBior1

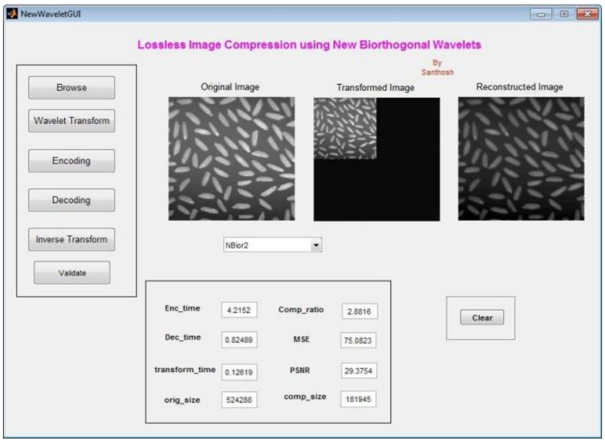

Fig. 4.6 Compression of 'rice.jpg' using NBior2

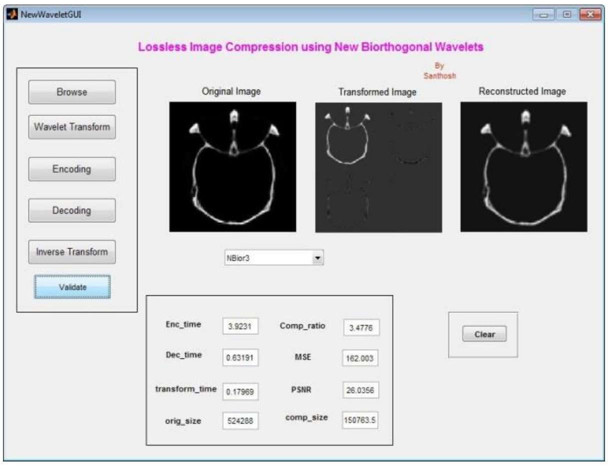

Fig. 4.7 Compression of 'ct.jpg' using NBior3

Fig. 4.8 Compression of 'pepper.jpg' using NBior4

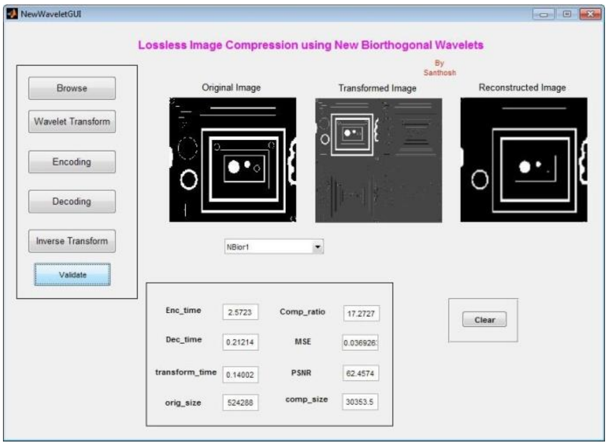

Fig. 4.9 Compression of 'blobs.jpg' using NBior1

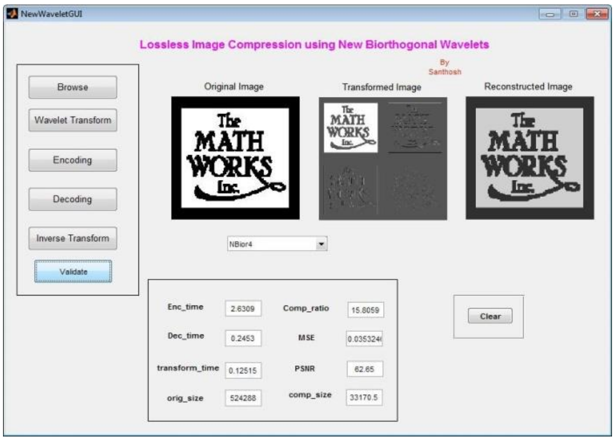

Fig. 4.10 Compression of 'logo.jpg' using NBior1

Table 4.2 PSNR values obtained with new conventional wavelets

PSNR (dB)						
	Lena.jpg	Rice.jpg	ct.jpg	Pepper.jpg	moon.tif	office_1.jpg
NBior1	31.6	32.81	33.30	30.95	34.27	37.56
NBior2	29.9	29.37	30.54	28.75	31.79	36.61
NBior3	26.7	27.01	26.03	24.95	27.62	34.17
NBior4	30.0	29.94	31.67	28.32	33.32	37.36

Table 4.3 PSNR values obtained with new conventional wavelets (contd. From Table 4.2)

PSNR (dB)						
	office_2.jpg	gantrycrane.png	circuit.tif	glass.tif	kids.tif	mandi.tif
NBior1	33.5	28.85	32.93	32.89	40.64	32.88
NBior2	32.1	27.45	30.91	31.73	39.35	29.75
NBior3	29.2	24.63	27.32	30.95	36.61	27.47
NBior4	33.1	29.83	31.07	30.43	39.78	31.47

Table 4.4 CR values obtained with new conventional wavelets

CR						
	Lena.jpg	Rice.jpg	ct.jpg	Pepper.jpg	moon.tif	office_1.jpg
NBior1	2.9	3.12	3.53	3.07	3.09	3.63
NBior2	2.9	2.88	3.53	3.08	3.10	3.64
NBior3	2.6	2.79	3.47	2.71	2.85	3.36
NBior4	2.6	2.75	3.44	2.69	2.82	3.36

Table 4.5 CR values obtained with new conventional wavelets (contd. From Table 4.4)

CR						
	office_2.jpg	gantrycrane.png	circuit.tif	glass.tif	kids.tif	mandi.tif
NBior1	3.0	3.01	2.94	3.46	3.93	3.09
NBior2	3.0	3.01	2.95	3.47	3.95	2.85
NBior3	2.7	2.82	2.55	3.11	3.63	2.72
NBior4	2.7	2.80	2.56	3.04	3.58	2.69

The new wavelet 'NBior1' is producing a PSNR around 33dB, while the 'CR' is around 3. On some images it is producing a 'PSNR' of even 40dB, 37dB and 34dB. With the new wavelet 'NBior2', the 'PSNR' is around 31dB and 'CR' is around 3. In the case of 'NBior3', the 'PSNR' is around 28dB and 'CR' is around 3. With 'NBior4', the 'PSNR' is around 32dB and 'CR' is around 3. The average values of 'PSNR', 'CR' and 'PC' [58] are given in table 4.6.

Table 4.6 Average 'PSNR', 'CR' and 'PC' values

	PSNR	CR	PC
NBior1	33.5	3.24	108.67
	31.5	3.20	101.14
NBior2	28.5	2.95	84.45
	32.2	2.92	94.33

The new conventional wavelets proposed in this chapter are compared with conventional wavelets. The 'PSNR', 'CR' and 'PC' values obtained using conventional and proposed wavelets are plotted in the figures 4.11, 4.12 and 4.13.

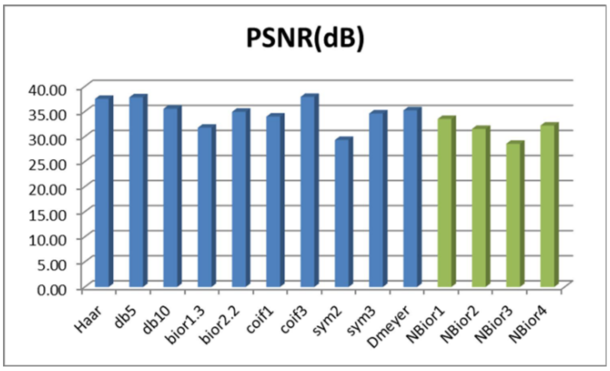

Fig. 4.11 'PSNR' values of conventional and proposed wavelets

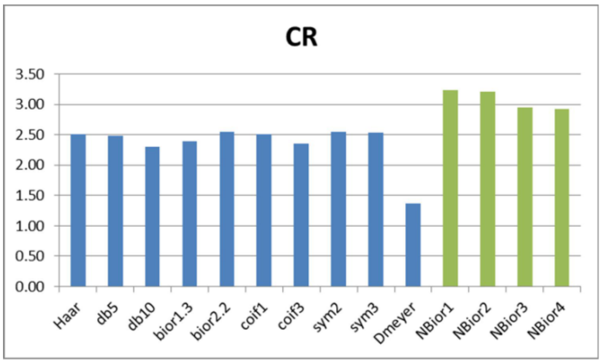

Fig. 4.12 'CR' values of conventional and proposed wavelets

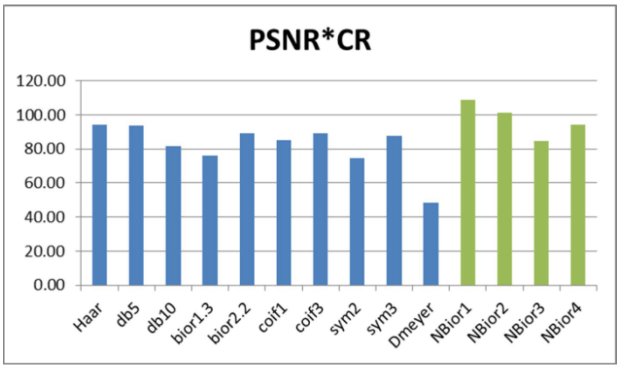

Fig. 4.13 'PSNR*CR' values of conventional and proposed wavelets

It is evident from Figures 4.11, 4.12 and 4.13 that the 'PSNR' is nearly in the same range for both conventional and proposed wavelets, and 'CR' is obviously large relative to conventional wavelets with proposed wavelets. The 'Nbior1" PSNR*CR' value is around 108, which is higher than that of all other planned and typical wavelets. In tables 4.7 and 4.8, the compression efficiency of new wavelets on binary images is presented. The 'PSNR' values on binary images are around 60dB with modern conventional wavelets and 'CR' is around 16 dB with new conventional wavelets.

Table 4.7 'PSNR' values obtained with new conventional wavelets on binary images

PSNR (dB)				
	blobs.png	circle.png	circbw.tif	logo.tif
NBior1	62.4	69.69	61.54	64.33
NBior2	60.2	66.21	56.85	56.96
NBior3	61.0	63.00	55.44	58.21
NBior4	61.7	67.95	59.91	62.65

Table 4.8 CR values obtained with new conventional wavelets on binary images

CR				
	blobs.png	circle.png	circbw.tif	logo.tif
NBior1	17.2	17.00	15.73	15.80
NBior2	17.2	17.00	15.73	15.80
NBior3	17.0	16.99	15.51	15.74
NBior4	17.1	17.00	15.67	15.80

5. CONCLUSION

The findings of the simulation presented above revealed that modern conventional wavelets' compression efficiency is superior to that of conventional wavelets. The 'PSNR' obtained is around 35dB with conventional wavelets and 'CR' is around 2.5. Although 'PSNR' is around 32dB with the recommended wavelets, and 'CR' is around 3. The 'PSNR' is marginally smaller than that of conventional wavelets for proposed wavelets, but the compression ratio is sufficiently higher such that the 'PSNR*CR' is 9 more than that of conventional wavelets. A little bit more than the actual wavelets are the planned wavelets. If the lifting version of the new conventional wavelets achieves much greater results, it is expected that these results will be equal to the lifting version of the latest conventional wavelets.

6. REFERENCES

1. Er. Kiran Bala, Varinderjit Kaur (2016). Advance Digital Image Compression Using Fast Wavelet Transforms Comparative Analysis With Dwt, International Journal Of Engineering Sciences & Research Technology. 5(7): pp. 1062-1069.

2. TAO LIU AND YALIN WU (2018). Multimedia Image Compression Method Based on Biorthogonal Wavelet and Edge Intelligent Analysis. SPECIAL SECTION ON GIGAPIXEL PANORAMIC VIDEO

WITH VIRTUAL REALITY. VOLUME 8, pp. 67354- 67365

3. J. Vinoth Kumar &Dr. C. Kumar Charlie Paul (2017). “A Survey on Wavelet Transform Techniques”, International Journal of Advanced Trends in Engineering and Technology, Page Number 72-73, Volume 2, Issue 1.

4. Khamees Khalaf Hasan, Mahmood Ali A. Dham and Shahir Fleyeh Nawaf (2018). Low Complexity Hardware Architectures for Wavelet Transforms: A Survey. IOP Conf. Series: Materials Science and Engineering, pp. 454. 012051 doi:10.1088/1757-899X/454/1/012051

5. Jean Hamilton, Matthew A. Nunes, Marina I. Knight & Piotr Fryzlewicz (2018) Complex-Valued Wavelet Lifting and Applications, Technometrics, 60:1, pp. 48-60, DOI: 10.1080/00401706.2017.1281846

6. Chen, D., Li, Y., Zhang, H. *et. al.* (2017). Invertible update-then-predict integer lifting wavelet for lossless image compression. *EURASIP J. Adv. Signal Process.* 2017, 8.

7. Prakash, Ashu. (2018). Wavelet and its Applications. International Journal of Scientific Research in Computer Science, Engineering and Information Technology. 3. Pp. 95-104. 10.32628/CSEIT183820.

Corresponding Author

Padmashri Dhanashire*

Research Scholar, Department of Electronics & Communication Engineering, Sri Satya Sai University of Technology & Medical Sciences, Sehore, M.P.